Dinovitser, Alex; Hamilton, Murray Wayne; Vincent, Robert Alan.
Stabilized master laser system for differential absorption lidar, *Applied Optics*, 2010; 49(17):3274-3281.

Stabilized master laser system for differential absorption lidar

Alex Dinovitser,* Murray W. Hamilton, and Robert A. Vincent

The University of Adelaide, Adelaide, SA 5005, Australia

*Corresponding author: alex.dinovitser@adelaide.edu.au

Received 2 March 2010; revised 11 May 2010; accepted 14 May 2010;
posted 18 May 2010 (Doc. ID 124863); published 3 June 2010

Wavelength accuracy and stability are key requirements for differential absorption lidar (DIAL). We present a control and timing design for the dual-stabilized cw master lasers in a pulsed master-oscillator power-amplifier configuration, which forms a robust low-cost water-vapor DIAL transmitter system. This design operates at 823 nm for water-vapor spectroscopy using Fabry–Perot-type laser diodes. However, the techniques described could be applied to other laser technologies at other wavelengths. The system can be extended with additional off-line or side-line wavelengths. The on-line master laser is locked to the center of a water absorption line, while the beat frequency between the on-line and the off-line is locked to 16 GHz using only a bandpass microwave filter and low-frequency electronics. Optical frequency stabilities of the order of 1 MHz are achieved.

OCIS codes: 140.3425, 280.1910.

1. Introduction

Differential absorption lidar (DIAL) is a spectroscopic technique for measuring the distribution of specific trace gas species in the atmosphere. Water vapor is a key trace gas since a knowledge of the atmospheric water-vapor concentration is vital for modeling meteorological phenomena and climate. It is now well known that water vapor plays a crucial role in both radiative and convective energy transfer through the atmosphere [1,2]. From the viewpoint of gaining sufficient data for weather and climate modeling, the main difficulty with water measurements in the atmosphere is the extreme and rapid variability of water concentrations compared to other gases [3]. Radiosondes are still the primary means of measuring atmospheric water vapor even though the recurrent costs are high, which limits the spatial and temporal extent of the data obtained. Despite major advances, satellite- and ground-based measurements based on spectral radiometry [4] and occultation [5] techniques still offer limited vertical resolutions.

Differential absorption lidar has good accuracy and vertical resolution, and has the potential for development as a low-cost lidar, which would alleviate the problems of horizontal and temporal resolution. Here we describe a laser transmitter system for DIAL, in the context of water vapor, but which is applicable to the detection of many other species. In DIAL, laser pulses at two wavelengths, tuned so that they encounter different absorption cross sections for the species being detected, are transmitted to the atmosphere. The relative intensities of backscattered light at the two wavelengths depend on the concentration of the absorbing species. Typically, the on-line laser is tuned to the center of a resonance, while the off-line wavelength is tuned away from a resonance where the absorption cross section is small. If the absorption cross sections are known, the concentration between these two ranges can be deduced after making certain assumptions about extinction and scattering [6]. Lidar detection of trace gases using Raman scattered light is an alternative method of profiling gas species in the atmosphere. However, DIAL can achieve a similar accuracy and detection limit with a power-aperture product that is more than an order of magnitude smaller than Raman

0003-6935/10/173274-08$15.00/0

[7]. This means that DIAL is more suitable for daytime applications, for power-critical space-based applications, and for cost-sensitive applications with lower power transmitters and smaller receivers. On the other hand, Raman lidar does offer the possibility of simultaneous temperature measurement [8], and the spectral purity and wavelength precision requirements on the laser are much less stringent than is the case for DIAL.

A number of DIAL systems have been developed for the profiling of water vapor [3,9–14]. Most of these systems rely on just one master laser, which is switched between the two wavelengths. However, it is difficult to switch the laser wavelength accurately between two wavelengths on a timescale of the order of 1 ms. The alternative with a single laser is to run the laser for several thousand pulses at one wavelength and then switch to the other wavelength, although this can lead to increased uncertainty if the concentration of the species being measured is changing rapidly. A different approach is to use two lasers that are tuned to the relevant wavelengths [14–17]. This greatly simplifies the problem of maintaining the lasers at the required wavelengths.

The problem of maintaining one laser at the absorption wavelength of the species of interest can be solved by either stabilizing the laser directly to the absorption line using a reference cell [14,15,18], or by using a wavemeter [10,17]. Next, the second laser wavelength needs to be maintained at a fixed wavelength or frequency difference from the first. In frequency terms, this difference should be at least 10 GHz for tropospheric water vapor measurements. Again, some have opted to achieve this using a wavemeter [10,17]. However, it is also straightforward to combine the two lasers and stabilize their beat frequency. In applications using extremely stable lasers, the beat frequency can be phase locked to a microwave reference oscillator, often an atomic clock [19] or a radio frequency oscillator [20]. In our application, extreme stability and phase coherence are not required. Methods of stabilizing the beat *frequency* to the reference oscillator have been reported. These have utilized a waveguide Mach–Zehnder interferometer so that a fixed frequency difference between the reference and the beat is achieved by locking to an interferometer fringe [21], or a microwave oscillator and a mixer, to downshift the beat frequency, and then using a low-pass electronic filter and power detector to generate a signal to stabilize the downshifted beat signal to zero frequency [18].

Our system uses two cw semiconductor master lasers, each continuously stabilized at their respective on-line and off-line wavelengths. Because this work is aimed at low-cost lidar, we have opted to stabilize the on-line wavelength to a water absorption cell, rather than use a wavemeter, and we use a novel method of stabilizing the beat frequency between the two lasers that does not require a microwave oscillator or a mixer, giving a significant reduction in cost. Because the lasers are operated in cw mode, acousto-optic switching is used to produce the laser pulses.

Semiconductor laser technology is also suited for the optical amplifier in a low-cost low-power system. The disadvantages of relatively low output power can be partly offset by having quite large pulse repetition rates of up to ~10 kHz. When the absorption line is too strong, a laser tuned to the side of the line can be employed [15]. This side-line wavelength can be stabilized at a precise offset from the center of the line with a straightforward extension of the techniques described in this paper. A simple calculation assuming a Lorentzian absorption line with width 1 GHz (HWHM) shows that the fractional change in absorption cross section is about 0.1% if the laser fluctuates by 3 MHz when tuned to the steepest part of the line. In both [15] and this work, a stability of better than 3 MHz is achieved.

2. DIAL Transmitter

Our DIAL master laser system uses two cw 40 mW Hitachi HL8325G laser diodes, operating near 823 nm. Pulses for amplification and transmission to the atmosphere are formed by acousto-optic modulators (AOMs). The remaining light (that is complementary to the pulsed beams) is used for wavelength stabilization of the master lasers. One laser is servo-locked to the wavelength of the peak of a water absorption line. The second is maintained at a fixed wavelength offset from the first by combining the two laser beams and stabilizing the frequency of the beat signal to the peak transmission of a microwave (RF) bandpass filter.

Figure 1 provides a simplified diagram of the entire lidar transmitter system. After passing through the AOM, each undeflected beam is coupled into a single-mode optical fiber. The pulsed beam that is Bragg scattered by the acoustic wave is directed to a beam splitter used as a combiner and then to the optical amplifier. Using the Bragg scattered wave, rather than the zeroth-order "straight-through" beam, as the basis for the pulse transmitted to the atmosphere ensures that the pulse from the master returns to zero. An added benefit of using the Bragg scattered beam in this way is that the AOM then contributes to the isolation of the master lasers from backreflections from the optical amplifier. The acoustic wave in each AOM is repetitively pulsed on for 1 μs with a period of 667 μs. The pulse length, which determines the transmitted pulse energy, is chosen as a trade-off between signal-to-noise and range resolution in the lidar return. This pulse width and period correspond to a range resolution of 150 m and a maximum range of 100 km. The effective maximum vertical range is very much less than this because of the relatively low transmitted pulse energy (~500 nJ). Indeed the data acquisition system only records for 50 μs after the pulse is transmitted, corresponding to a maximum range of about 7 km. Vertical resolution could be improved by reducing the pulse width, but this would reduce pulse energy and signal-to-noise ratio,

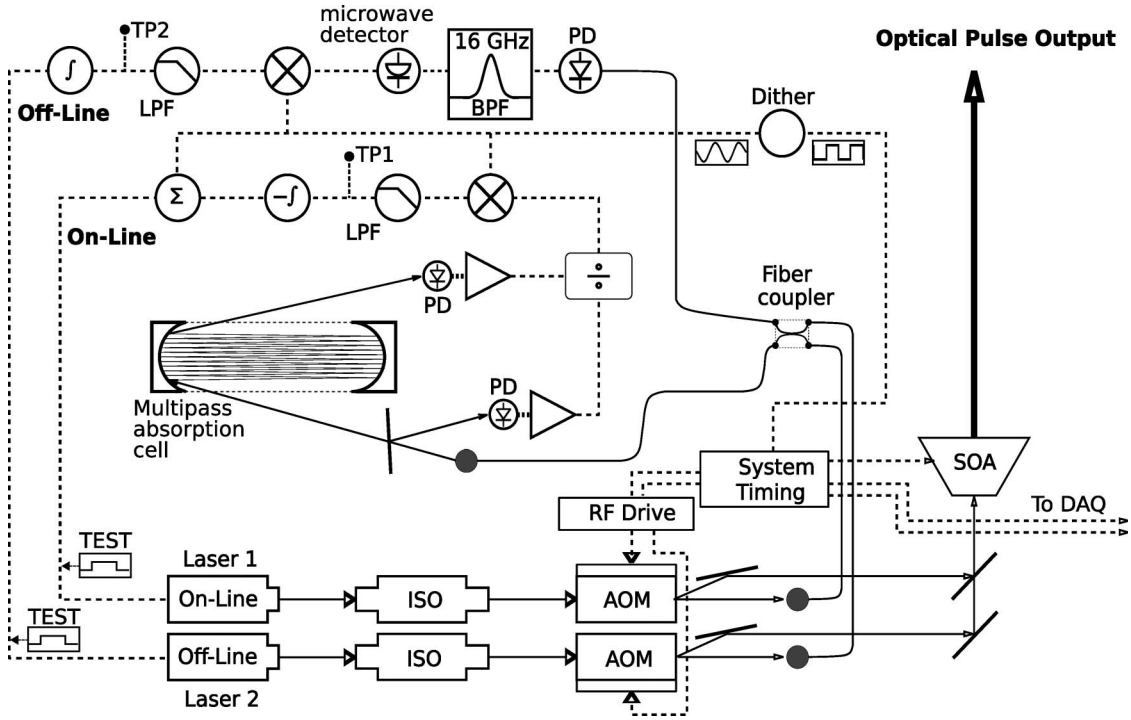

Fig. 1. Differential absorption lidar laser stabilization system showing optical paths (solid lines) and electronic signals (dashed lines). AOM, acousto-optic modulator; SOA, semiconductor optical amplifier; ISO, Faraday optical isolator; DAQ, data acquisition; PD, photodiode; LPF, low-pass filter; BPF, bandpass filter; TP, test point. The blocks labeled TEST indicate the points at which step voltages are used to test the response of the servo loops, as discussed in the text. The gray circles represent fiber coupling lenses.

as well as compromising the maximum vertical range because of background light. The pulse repetition rate could be considerably higher without introducing range ambiguities, but in our case is limited by the data acquisition system.

To achieve reasonably reproducible tuning characteristics and longitudinal mode stability, light from each laser diode passes through two Faraday isolators, together providing 60 dB of optical isolation. Each laser operates in a single longitudinal mode and provides a mode-hop-free tuning range of more than 200 GHz. They operate in several discrete regions over a wavelength band from 820 to 834 nm. Device selection is necessary to have two lasers that tune to the same wavelength range. Of 15 devices, we found three that would tune continuously, and repeatably, over a range from 822.6 to 823.4 nm. The ability to tune over this range has remained unchanged over three years, and only requires that the diode temperature and current are stabilized near particular values. The tuning of these diodes is subject to hysteresis when mode hops occur. Because of this, it is necessary that the desired temperature and current be approached in a certain direction. In establishing these properties, an optical spectrum analyzer proves useful. The optical amplifier is a Sachertechnik TA830 tapered amplifier with injection current pulsed synchronously with the arrival of the master laser pulses of alternating wavelength. Its rated maximum output power is 500 mW.

A. On-Line Master Laser Control System

The zeroth-order on-line laser beam after the AOM is coupled into a single-mode optical fiber, and then to a 50:50 fiber coupler, which serves as both a splitter and a combiner. An important function of the fiber is to isolate the alignment of the beams around the AOMs and isolators from alignment at the absorption cell. One output port of the coupler directs the light to a multipass absorption cell with a 30 m path length, a ratiometric detector, and a feedback system to control laser current and wavelength. Our multipass cell is a homemade variant of a Herriot cell, where the light is coupled into the space between the mirrors via a small periscope. After 66 traversals of the space between the mirrors, the beam encounters the periscope again and is coupled out of the cell.

A dither modulation at 1.5 kHz is introduced via the on-line laser current control so that the laser has a peak-to-peak frequency modulation of 500 MHz. Phase-sensitive detection of the resulting amplitude modulation at the output of the vapor cell, when the laser is tuned through a water resonance, provides an error signal in order to keep the laser locked to the water resonance peak. However, there are unwanted sources of amplitude modulation with changing laser wavelength. First, the dither of laser injection current also modulates the laser power. Second, the multiple-beam interference fringes due to reflections within the fiber splitter have a greater contrast than many water absorption lines. By comparing the optical

power entering the vapor cell with the power transmitted through it, the ratiometric detector eliminates both of these sources of error. In the output of the ratiometric detector, these variations are reduced to below the level of the electronic noise.

Two other less significant sources of wavelength error have not been dealt with. First, there is some multiple-beam interference due to the water-vapor cell itself, because there is a small amount of overlap of the laser spots on the mirrors. Some light at the mirrors is scattered into paths that effectively shortcut one or more of the passes in the cell, and this is manifested as fringes at the output of the ratiometric detector, with a free spectral range corresponding to the mirror separation. In our case, these fringes are more than an order of magnitude weaker than the absorption line at 822.9 nm that we use, and cause negligible offset error in the stabilization to the center of the water line. For weaker lines, however, this could be a major concern. Second, the pulses transmitted to the sky are shifted in frequency from the absorption line center by the 80 MHz acoustic frequency of the AOM. In the lower troposphere, where the water absorption lines are at least 2 GHz wide (HWHM), this introduces a negligible systematic error for our application (<0.3% difference between the peak and actual absorption cross sections).

To minimize the cost and component count of the system, we use a single fiber coupler. This means that the off-line laser also passes through the absorption cell. However, because its wavelength is not modulated, it does not affect the on-line control system. Although a 16 GHz beat signal between the on-line and off-line lasers is also present at the water-vapor cell, the low-speed photodiodes at the absorption cell do not respond to modulation at this frequency.

B. Off-Line Master Laser Control System

The off-line master laser is isolated, passed through an AOM, and coupled into the fiber coupler in the same way as the on-line laser. The second output from the fiber coupler goes to a photodiode (New Focus Model 1481-S) which has a frequency response from DC to 25 GHz. This diode detects the beat frequency between the two lasers. We have chosen a fixed frequency offset between the on- and off-line lasers of 16 GHz. Since the on-line master laser already includes a dither, the beat signal around 16 GHz also has a frequency modulation amplitude of 500 MHz at 1.5 kHz. The bandpass filter, with a center frequency of 16 GHz and a −3 dB bandwidth of 500 MHz, converts this frequency modulation to an amplitude modulation whose phase depends on which side of the filter's transfer function the beat is tuned to. The microwave power is detected by a tunnel diode detector (Herotek DT2018), which has a bandwidth much greater than 1.5 kHz, so that phase sensitive amplification of the dither component of the microwave power can be used to generate an error signal. This is integrated and fed back to the off-line laser injection current controller. Thus, the off-line control system locks the frequency difference of the lasers to the zero crossing of the derivative of the bandpass filter's transfer function, in a similar way to the stabilization used for the on-line laser.

There are two lock points for the off-line laser, one on each side of the absorption line. These are easily distinguishable when setting up the system. Note that there are only two such points, in contrast to [18], where there are four, because we dispense with a microwave oscillator.

Obtaining a different frequency offset (from 16 GHz) between the lasers is simply a matter of picking a bandpass filter with passband centered at the desired offset frequency. The bandwidth should be reasonably narrow, and the filter transfer function should not have ripple or a wide flat region in the passband. Of course, the photodiode that detects the beat signal needs to have a sufficiently large bandwidth—this will be the limiting factor in practice. Photodiodes with bandwidth of up to 100 GHz are obtainable. The price of microwave components tends to increase with increasing frequency, and we have chosen the value 16 GHz as a compromise between cost and the need to make sure that the off-line laser is tuned sufficiently far into the wings of the water absorption line.

3. System Timing

For water vapor in the lower troposphere, the linewidth of the molecular resonance at 822.9 nm is dominated by pressure broadening and ranges from about 5 GHz at sea level to about 2 GHz at the highest altitude at which we expect to be able to measure water-vapor concentrations with a transmitted pulse energy of 500 nJ (about 4 km). The smaller of these linewidth values imposes a constraint on the linewidth of the on-line master laser, which should be less than 100 MHz [22]. However, the amplitude of the frequency dither applied to the on-line master laser is 500 MHz. To get around this difficulty, we synchronize the extraction of the optical pulses by the AOMs with the zero crossings of the dither signal (Fig. 2). This ensures that the laser frequency within the pulses is consistent from pulse to pulse. Provided the pulse is short compared to the dither period, the frequency chirp within the pulse can be neglected. In our system, the pulse length is 1 μs and the dither period is 1333 μs, resulting in an optical frequency chirp of less than 1 MHz.

The output pulse can be set to any phase of the dither signal, but there is an advantage to keeping it close to the zero crossing. When the optical path is switched out of the cw beam by the AOM to form the output pulse, a transient will appear on the output of the ratiometric detector, which, although short in duration, will disturb the feedback control loop at the integrator. If this transient is timed to coincide with the zero crossing of the dither signal, the transient will not be propagated through the control system. In other words, the transient impulse due to optical switching will be attenuated by the lock-in

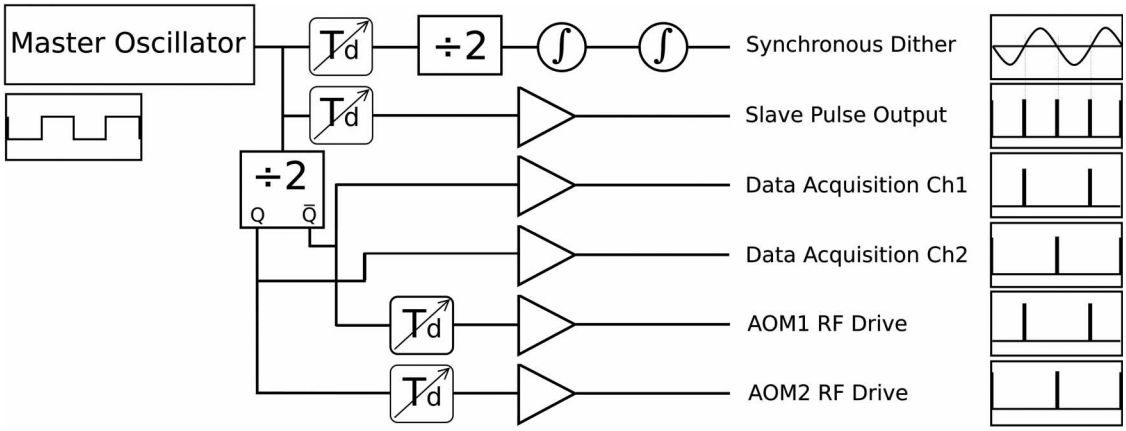

Fig. 2. System timing coordinates the optical switching (AOM), electronic switching, dither, and data acquisition. The adjustable delays (Td) compensate for the response times of the electronic and optical components, such as the finite time for acoustic signals to propagate through the AOMs (~400 ns) to effect the optical switching. In addition, the delays ensure that the data acquisition system is triggered ~5 μs before the laser pulses are transmitted, to enable background signal levels to be measured. The pulse lengths are controlled by monostable multivibrators (HC4538), that are not shown explicitly.

(which is an analogue multiplier), if it coincides with an instantaneous zero reference.

4. Wavelength Stability Measurements

Here we present the wavelength stability, which is one of the critical characteristics for any DIAL system, as well as show the transient behavior of the system. Some DIAL measurements are also presented to demonstrate the reliability of the stabilization system.

To measure the residual optical frequency fluctuations, our procedure is as follows. First we apply a step perturbation to the on-line laser while measuring the change in the beat frequency, with the feedback loops open. This enables us to relate the magnitude of the error signals observed at TP1 and TP2 (see Fig. 1) to the size of the frequency excursion.

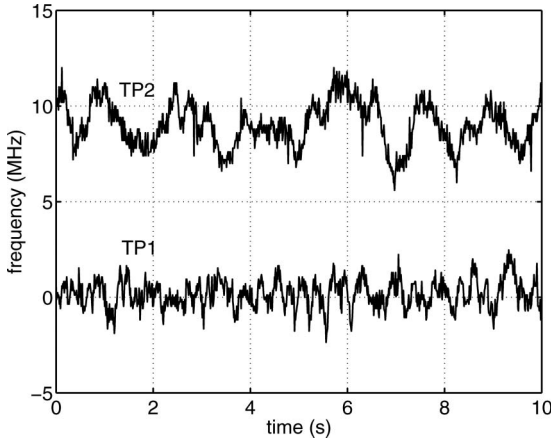

Fig. 3. Laser wavelength variability measured from the error signals at TP1 and TP2, with the feedback loops closed. TP1 shows the fluctuations in the on-line laser frequency, and TP2 shows those for the difference frequency. The signals shown are the voltages measured at the respective test points, scaled as described in the text so that the vertical axis is in frequency units. The vertical separation between the traces is an arbitrary DC shift introduced for clarity.

Next, the feedback loops are closed and the noise at TP1 and TP2, as shown in Fig. 3, is measured. In this figure, the conversion relating voltage to frequency has been applied so that the vertical scale represents the frequency excursion. From the measurement at TP2, we obtain a relative frequency variability (RMS) between the lasers of 1.2 MHz, and from that at TP1, an RMS value of 0.7 MHz for the fluctuation in the frequency of the on-line laser.

Here we measure noise that has frequency components that are mostly greater than the reciprocal of the feedback loop time constants (both ~1 s). Frequency fluctuations on a time scale significantly shorter than 1 s are uncorrected by the feedback. Thus, the noise at TP2 is the sum of uncorrelated contributions from both the on-line and off-line lasers. There are also contributions from the electronics. These time constants were gauged from the

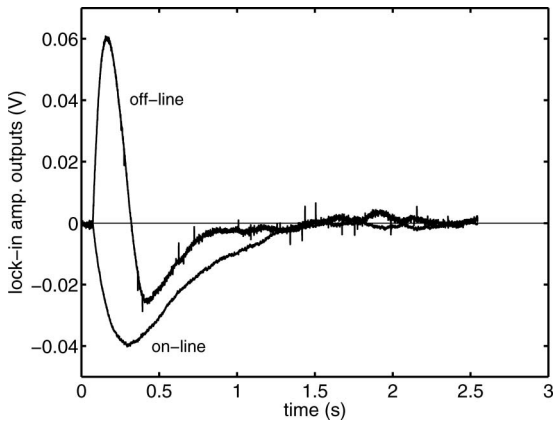

Fig. 4. Response of the control loops to small-signal step perturbation at the on-line laser. The response of the on-line control system acts to cancel the effect of the perturbation as the area under the error-signal curve is equal to the step amplitude. The instantaneous shift in the beat frequency also produces an error signal in the off-line control signal.

transient behavior of the error signals when a step perturbation was applied to the on-line laser, while both feedback loops were closed. A step voltage injected directly into the on-line laser diode injection current controller, at one of the points labeled TEST in Fig. 1, produced an ~50 MHz instantaneous frequency shift in the on-line master laser and the beat note simultaneously. The response of both control systems acts to cancel the frequency shift. The responses at the test points TP1 and TP2 to a perturbation at the on-line laser are illustrated in Fig. 4. The relaxation times for the signals are both ~1 s, and these are the loop time constants.

The off-line control system responds to the beat frequency shift, even though there is no perturbation to the off-line wavelength; however, the output from the off-line integrator returns to its original value. It is interesting to note in Fig. 4 that, even though the optical and RF beat frequency perturbation are in the same direction, the instantaneous responses of the two control systems are in opposite directions. This is because the integration constants of the two control loops are of the opposite sign because the water absorption behaves like a band-stop filter, while the 16 GHz filter is a bandpass filter.

The effect of multiple-beam interference in the optical path between the on-line laser and the photodetector after the multipass absorption cell is to superpose small interference fringes on the water absorption profile. Such interference is rather temperature sensitive. This can give rise to an offset in the locking point for the on-line laser, which, in turn, contributes to the fluctuations of the beat frequency between the two lasers, on a time scale of several seconds. We observe these fluctuations when the off-line laser is unlocked and the on-line laser is locked; when both loops are locked, they are present but not directly visible. Such fluctuations are of a similar order of magnitude to the RMS fluctuations shown in Fig. 3, i.e., about 1 MHz. Thus, this source of error is reduced to an acceptable level, also.

Table 1. Maximum Fractional Absorption for Water at 822.92 nm with Relative Humidity 54%

	Calculated from RH	Measured
Amplified	0.1279	0.1224
Master only	0.1282	0.1301

An important point is that these results were obtained at a sampling rate of 100 samples/s, capturing only the low-frequency perturbations up to 50 Hz. Faster frequency fluctuations were also present but at a much lower level, evidenced by measurements of the 16 GHz beat spectrum. A full measurement of the laser spectra is required to characterize the rapid fluctuations that contribute to the spectral wings. This knowledge is critical in DIAL because, if the spectral wings of the on-line laser extend well into and beyond the wings of the absorption spectrum, the effective absorption cross section is reduced from that which would we obtain for a perfectly monochromatic laser tuned to line center. Such a reduction leads to a systematic error in the retrieved water concentration. This can be the case even if the width at half-maximum of the laser spectrum is much less than that of the absorption spectrum, as the former may have significantly more power in the far wings than Lorentzian-or Gaussian-shaped spectra. This is especially true of diode lasers, and others that have very broad gain bandwidths.

To illustrate the problem, we show in Table 1 measurements of the maximum fractional absorption in the multipass cell as the on-line master laser (with and without amplification) is tuned through the line at 822.92 nm. The calculated absorption is that which would be expected based on a measurement of the humidity by a capacitive sensor that was calibrated against the saturated vapor pressure over a saturated salt solution (magnesium nitrate) [23,24]. The relative humidity (RH) was 54% and the temperature was 296 K. The absorption cross section is deduced from the HITRAN database [25]. The ab-

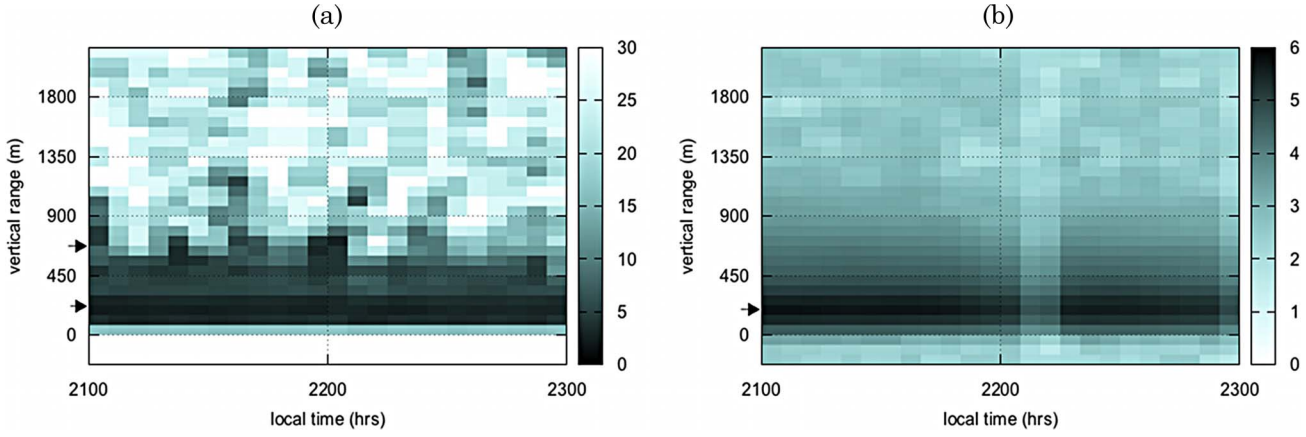

Fig. 5. (Color online) (a) Measurements of water vapor mixing ratio (in grams per kilogram) using the DIAL, and (b) the raw backscatter signal for the off-line wavelength, showing the height to which aerosol scattering is seen. In (a), the arrows on the left-hand scale indicate the approximate boundaries of height range for which there is a signal-to-noise ratio greater than 1. In (b), the arrow on the scale indicates the height of maximum signal, which is the point at which the transmitted beam fully intersects the field of view of the receiving telescope.

sorption cross section of the master laser is slightly larger than expected, but this is within the measurement uncertainty. The absorption cross section of the amplified light is about 5% less than expected, and this reduction is attributable to the amplified spontaneous emission from the optical amplifier, and the resulting lack of spectral purity. The two values for expected absorption are different because the temperature and humidity changed slightly between the measurements. Such a measurement can be made straightforwardly each time the lidar is operated, in order to establish the effective on-line absorption cross section.

As a demonstration that this master laser system works reliably, we include DIAL measurements in Fig. 5. These data were obtained with the lidar pointing at the zenith from the Adelaide central business district, over two hours on the evening of 22 March 2010. The time shown is local time. Figure 5(a) shows the water-vapor mixing ratio in grams per kilogram and Fig. 5(b) shows the base-ten logarithm of raw return signal for the off-line wavelength. The data were oversampled in time at 50 ns intervals by the data acquisition system, and averaging over 500 ns has been applied, corresponding to 75 m intervals on the vertical scale. (The transmitted pulse width is 1 μs, so that the true range resolution is 150 m.) The data are also averaged over 5 min intervals, in which there were approximately 1.5×10^5 transmitted pulses at each wavelength. In Fig. 5(a), the signal to noise falls to 1, above about 700 m. Figure 5(b) partly explains this rather low maximum range; the return from the aerosols has fallen to the background signal level by about 1 km. The on-line signal falls somewhat faster, due to absorption, and when this signal has fallen to the background, meaningful measurement of mixing ratio is no longer possible. This shallow depth of the aerosol scatterers is typical for this location. The vertical band of low signal in Fig. 5(b), at about 2210 h, was caused by the alignment between master and slave drifting. This was readjusted without affecting the lock of the master laser system. There is a corresponding "hole" of noisy data in Fig. 5(a) at about the same time. The receiving telescope had a diameter of 40 cm, and the on-line wavelength was 822.92 nm.

5. Conclusion

We describe a low-cost master laser system for DIAL using a separate master laser for each wavelength. A synchronous dither and timing system locks the wavelength of the transmitted pulse to the desired wavelength. The wavelength stability shows a RMS variability of less than 1 MHz over 10 min. The system design lends itself to other types of laser diodes and optical amplifiers, and also to multiple off-line wavelengths.

This work was funded by the Australian Research Council and the Australian Bureau of Meteorology. Contributions by K. Bae, C. Baer, A. Heitmann, and P. Moran are gratefully acknowledged.

References

1. K. Minschwaner and A. E. Dessler, "Water vapor feedback in the tropical upper troposphere: model results and observations," J. Climate **17**, 1272–1282 (2004).
2. W. Ingram, "On the robustness of the water vapor feedback: GCM vertical resolution and formulation," J. Climate **15**, 917–921 (2002).
3. S. Pal, A. Behrendt, H. Bauer, M. Radlach, A. Riede, M. Schiller, G. Wagner, and V. Wulfmeyer, "3-dimensional observations of atmospheric variables during the field campaign COPS," IOP Conf. Ser.: Earth Environ. Sci. **1**, 012031 (2008).
4. V. Wulfmeyer, H. Bauer, P. Di Girolamo, and C. Serio, "Comparison of active and passive water vapor remote sensing from space: an analysis based on the simulated performance of IASI and space borne differential absorption lidar," Remote Sens. Environ. **95**, 211–230 (2005).
5. S. Heise, J. Wickert, G. Beyerle, T. Schmidt, and Ch. Reigber, "Global monitoring of tropospheric water vapor with GPS radio occultation aboard CHAMP," Adv. Space Res. **37**, 2222–2227 (2006).
6. A. Ansmann and J. Bosenberg, "Correction scheme for spectral broadening by Rayleigh scattering in differential absorption lidar measurements of water vapor in the troposphere," Appl. Opt. **26**, 3026–3032 (1987).
7. V. Wulfmeyer and J. Bosenberg, "Ground-based differential absorption lidar for water-vapor profiling: assessment of accuracy, resolution, and meteorological applications," Appl. Opt. **37**, 3825–3844 (1998).
8. A. Behrendt, T. Nakamura, M. Onishi, R. Baumgart, and T. Tsuda, "Combined Raman lidar for the measurement of atmospheric temperature, water vapor, particle extinction coefficient, and particle backscatter coefficient," Appl. Opt. **41**, 7657–7666 (2002).
9. D. Bruneau, P. Quaglia, C. Flamant, M. Meissonnier, and J. Pelon, "Airborne lidar LEANDRE II for water-vapor profiling in the troposphere. I. System description," Appl. Opt. **40**, 3450–3461 (2001).
10. A. R. Nehrir, K. S. Repasky, J. L. Carlsten, M. D. Obland, and J. A. Shaw, "Water vapor profiling using a widely tunable, amplified diode-laser-based differential absorption lidar (DIAL)," J. Atmos. Ocean. Technol. **26**, 733–745 (2009).
11. J. L. Machol, T. Ayers, K. T. Schwenz, K. W. Koenig, R. M. Hardesty, C. J. Senff, M. A. Krainak, J. B. Abshire, H. E. Bravo, and S. P. Sandberg "Preliminary measurements with an automated compact differential absorption lidar for the profiling of water vapor," Appl. Opt. **43**, 3110–3121 (2004).
12. H. Schwarzer, A. Börner, A. Fix, B. Günther, H-W. H., M. Raugust, F. Schrandt, and M. Wirth, "Development of a wavelength stabilized seed laser system for an airborne water vapour lidar experiment," Proc. SPIE **6681**, 66810H (2007).
13. E. V. Browell, S. Ismail, and W. B. Grant, "Differential absorption lidar (DIAL) measurements from air and space," Appl. Phys. B **67**, 399–410 (1998).
14. M. Wirth, A. Fix, P. Mahnke, H. Schwarzer, F. Schrandt, and G. Ehret, "The airborne multi-wavelength water vapor differential absorption lidar WALES: system design and performance," Appl. Phys. B **96**, 201–213 (2009).
15. G. J. Koch, J. Y. Beyon, F. Gibert, B. W. Barnes, S. Ismail, M. Petros, P. J. Petzar, J. Yu, E. A. Modlin, K. J. Davis, and U. N. Singh, "Side-line tunable laser transmitter for differential absorption lidar measurements of CO_2: design and application to atmospheric measurements," Appl. Opt. **47**, 944–956 (2008).
16. K. Ertel, H. Linné, and J. Bösenberg, "Injection seeded pulsed Ti:sapphire laser with novel stabilization scheme and capability of dual-wavelength operation," Appl. Opt. **44**, 5120–5126 (2005).

17. H. R. Khalesifard, A. Fix, G. Ehret, M. Schiller, and V. Wulfmeyer, "Fast-switching system for injection seeding of a high-power Ti:sapphire laser," Rev. Sci. Instrum. **80**, 073110 (2009).
18. S. Schilt, R. Matthey, D. Kauffmann-Werner, C. Affolderbach, G. Mileti, and L. Thévenaz, "Laser offset-frequency locking up to 20 GHz using a low-frequency electrical filter technique," Appl. Opt. **47**, 4336–4344 (2008).
19. L. Hollberg, S. Diddams, A. Bartels, T. Fortier, and K. Kim, "The measurement of optical frequencies," Metrologia **42**, S105–S124 (2005).
20. J. Appel, A. MacRae, and A. I. Lvovsky, "A versatile digital GHz phase lock for external cavity diode lasers," Meas. Sci. Technol. **20**, 055302 (2009).
21. U. Schünemann, H. Engler, R. Grimm, M. Weidemüller, and M. Zielonkowski, "Simple scheme for tunable frequency offset locking of two lasers," Rev. Sci. Instrum. **70**, 242–243 (1999).
22. V. Wulfmeyer and C. Walther, "Future performance of ground-based and airborne water-vapor differential absorption lidar. II. Simulations of the precision of a near-infrared, high-power system," Appl. Opt. **40**, 5321–5336 (2001).
23. World Meteorological Organization, "Measurement of humidity," in *Guide to Meteorological Instruments and Methods of Observation* (World Meteorological Organization, 2008), pp. 1.4–25.
24. A. Apelblat, "The vapour pressures of water over saturated aqueous solutions of barium chloride, magnesium nitrate, calcium nitrate, potassium carbonate, and zinc sulfate, at temperatures from 283 K to 313 K," J. Chem. Thermodyn. **24**, 619–626 (1992).
25. L. S. Rothman, I. E. Gordon, A. Barbe, D. C. Benner, P. F. Bernath, M. Birk, V. Boudon, L. R. Brown, A. Campargue, J.-P. Champion, K. Chance, L. H. Coudert, V. Danaj, V. M. Devi, S. Fally, J.-M. Flaud, R. R. Gamache, A. Goldmanm, D. Jacquemart, I. Kleiner, N. Lacome, W. J. Lafferty, J.-Y. Mandin, S. T. Massie, S. N. Mikhailenko, C. E. Miller, N. Moazzen-Ahmadi, O. V. Naumenko, A. V. Nikitin, J. Orphal, V. I. Perevalov, A. Perrin, A. Predoi-Cross, C. P. Rinsland, M. Rotger, M. Šimečková, M. A. H. Smith, K. Sung, S. A. Tashkun, J. Tennyson, R. A. Toth, A. C. Vandaele, and J. Vander Auwera, "The HITRAN 2008 molecular spectroscopic database," J. Quant. Spectrosc. Radiat. Transfer **110**, 533–572 (2009).